The Kinetics of Monazomycin-induced Voltage-dependent Conductance

I. Proof of the Validity of an Empirical Rate Equation

ROBERT U. MULLER, GARY ORIN, and CHARLES S. PESKIN

From the Department of Physiology, Downstate Medical Center, State University of New York, Brooklyn, New York 11203 (Robert U. Muller and Gary Orin), and Courant Institute of Mathematical Sciences, New York University, New York, New York 10012 (Charles S. Peskin).

ABSTRACT Monazomycin (a positively-charged, polyene-like antibiotic) induces a strongly voltage-dependent conductance in thin lipid membranes when added to one of the bathing solutions. We show here that the kinetics of conductance changes after a step of membrane potential are only superficially similar to the kinetics of the potassium gating system of squid giant axons, in that the beginning of conductance increases are growth functions of the time, as opposed to power functions of the time. We find that the rate constant (reciprocal of the time constant) of the growth varies with the ~2.6 power of the monazomycin concentration. The rate constant also varies exponentially with membrane potential such that an e-fold change is associated with a 10–11 mV change of membrane potential. We show that solutions of a simple differential equation are able to reproduce the actual conductance changes almost exactly. In the accompanying paper (Muller and Peskin. 1981. *J. Gen. Physiol.* **78**:201–229), we derive the differential equation from a molecular model and use the theoretical equation so obtained to investigate the gating current of this system and to predict an interesting form of memory.

INTRODUCTION

Monazomycin-treated thin lipid membranes exhibit a voltage-dependent, time-varying conductance to univalent cations whose kinetics resemble those of the potassium gating system of squid giant axons. After a positive-going[1] step of membrane potential, both conductances increase in an S-shaped fashion to a steady-state level (g_∞). For both, the magnitude of the steady-state conductance is, over a wide voltage range, a steep exponential function of the potential (a 4–5-mV change leads to an e-fold conductance shift).

[1] As usual, the potential of the extracellular fluid is taken as zero for the axon. Sign conventions for the monazomycin system are given in the Materials and Methods section of this paper.

J. GEN. PHYSIOL. © The Rockefeller University Press · 0022-1295/81/08/0171/30 $1.00 171
Volume 78 August 1981 171–200

Finally, after negative-going voltage steps, each conductance decays to a lower steady-state level over an uninflected time-course.

The dependence of g_∞ on membrane potential (V) and monazomycin concentration in the aqueous solution ([Mon]) has already been described (Muller and Finkelstein, 1972*a* and *b*). Here, we focus on the kinetics of the conductance; that is, we are interested in the details of the trajectory that the conductance (g) follows in going from an initial to a final steady state. Perhaps the most interesting outcome of this analysis is the (experimentally realized) prediction that a form of memory is implicit in an understanding of the response to single voltage steps.

We will proceed in the following manner: In this paper, we will first show that the exact form of monazomycin conductance changes cannot be fit by the Hodgkin and Huxley (1952) scheme for the potassium conductance. We then demonstrate that a simple differential equation (Eq. 6), treated initially as empirical in nature, can generate solutions that virtually superimpose on actual voltage clamp records. The bulk of the rest of this paper will be used to find how the constants in Eq. 6 vary with membrane potential and monazomycin concentration.

In the accompanying paper (Muller and Peskin, 1981) (paper II) we show that Eq. 6 can be derived from a variety of molecular models; we will use the data set out here to decide which of the models are compatible with the actual conductance changes. We will then describe the memory process alluded to above, show some of its characteristics, and speculate on how a monazomycin-like molecule in the right places in the nervous system could change ordinary chemically transmitting synapses into "plastic" synapses.

A few words about our general orientation are required as background. We will assume in these papers that the monazomycin-induced conductance is based on the formation of ion-permeant channels. The existence of current pulses at very low total conductance (Muller and Andersen, 1975; Bamberg and Janko, 1976; Muller and Andersen, manuscript in preparation) and the characteristics of the noise spectrum of monazomycin modified membranes (Kolb, 1979; Moore and Neher, 1976; Wanke and Prestipino, 1976) constitute virtual proofs of mechanism. We will make use of the single channel measurements from a companion study (Muller and Andersen, manuscript in preparation) when we do our numerical computations. Beyond this, we will also imagine that the channels are of a single type and that they are individually ohmic when the membrane is bathed by identical solutions. If both of these statements were exactly true, it would mean that our (chord) conductance measurements would simply reflect the number of channels extant in the membrane at any moment. Actually, as Muller and Andersen (manuscript in preparation) report, there are at least three channel varieties. However, in the voltage range used in these studies, almost all of the conductance is due to one type, so that our picture is not much in error. With regard to the ohmic property, this certainly seems to be the case when the membrane potential is <100 mV and is very nearly true even ≤ 160 mV, well in excess of the largest potentials we will use here. Macroscopic measurements (Muller and Finkelstein, 1972 *a*) also indicate that the conductance is instantaneously ohmic. We

conclude that it is reasonable to equate the moment-to-moment conductance with the number of channels. This means that at constant membrane potential, the current changes that we measure directly reflect changes in the size of the channel population.

MATERIALS AND METHODS

A. Preparation of Membranes

Nearly all experiments were done on membranes symmetrically bathed by unbuffered 0.1 M KCl. The membranes were made by the brush technique of Mueller et al. (1963) across a 1-mm diameter (0.8 mm^2) hole in a thin Teflon partition. Many experiments were done at ambient temperature, which ranged between 20° and 30°C, but on occasion a water-jacketed bath was used and the temperature of the KCl solutions was directly monitored.

The state of the membrane was determined visually; a film was used only after it had a homogeneous black appearance. A further requirement was that the unmodified membrane conductance be $\leq 10^{-10}\ \Omega^{-1}$. Capacitance measurements were sometimes made to confirm the thin state of the membrane; the specific capacity of the black region was always $\sim 4 \times 10^{-7}\ F \cdot cm^{-2}$.

In most cases, membranes were painted from a solution of 1% bacterial phosphatidylglycerol (PG) (Supelco, Inc., Bellefonte, Pa.) plus 1% cholesterol (Eastman Kodak Co., Rochester, N. Y.; recrystalized twice from ethanol) in *n*-decane (Supelco, Inc., or Analabs, Inc., Foxboro Co., New Haven, Conn.). Bacterial phosphatidylethanolamine (PE) (Supelco, Inc.) was also used, as were other solvents (*n*-octane, *n*-dodecane). The behavior of the monazomycin-induced conductance was not changed by varying the solvent. Cholesterol was sometimes omitted. Composition of the membrane-forming solution will be specified only when it differed from the 1% PG + 1% cholesterol in decane mixture. (Although we have not done extensive work with lipids other than PG and PE, the general nature of the monazomycin kinetics appears the same with phosphatidylcholine and phosphatidylserine membranes.)

Monazomycin was the generous gift of Dr. Yonehara and Dr. Otake of The Institute for Applied Microbiology, University of Tokyo, Tokyo. The antibiotic was added to only one compartment from an aqueous solution whose concentration was between 30 and 2,000 μg/ml. The final concentration in the bath was between 2.5×10^{-7} g/ml and 9×10^{-6} g/ml. (The molecular weight of monazomycin is ~1,200 [Akasaki et al., 1963].) In the higher concentration stock solutions (>1,000 μg/ml) an off-white precipitate formed after a month or two. We did not observe any change in the potency of the solution when this happened.

B. Electrical Measurements

The variable of primary interest in these experiments is the monazomycin-induced (chord) conductance. Because the two solutions bathing our membranes were identical ([Mon] ≈ 0), the conductance (g) is defined as:

$$g = \frac{I}{V},$$

where I is the ionic current that flows through the membrane and V is the voltage difference imposed across the membrane. Voltage steps were applied and the current measured by a standard two-electrode voltage clamp. Calomel electrodes in series with saturated KCl bridges were used to make contact with the bathing solutions.

We make our electrical sign conventions with respect to the asymmetrical distribution of monazomycin. The compartment that contains the antibiotic is designated "*cis*." The other, "*trans*," compartment is maintained at virtual ground by the voltage-clamp circuit. Thus, a positive voltage difference means the *cis* compartment is positive with respect to the *trans*. Positive current flows from *cis* to *trans*. Conductance measurements were restricted to the range $2 \times 10^{-6} > g > 10^{-10}\ \Omega^{-1}$.

For the work reported here, we found it extremely helpful to use a logarithmic amplifier (model 755N or 755P; Analog Devices, Inc., Norwood, Mass.). The output of the current-to-voltage converter of the voltage clamp is used to drive the log amplifier (with a low-pass filter, described below, interposed between the two devices).

Either log amplifier yields a linear change in output voltage for an exponential voltage increase at the input over the approximate range from 10^{-4} to 10 V, scaled so that a 10-fold increase produces a 1.0-V output change. An input of 100 mV corresponds to an output of $V = 0$. The sole difference in the P and N modules lies in the input voltage polarity which is acceptable; the N module operates with positive inputs, the P with negative. We used one or the other of these as dictated by the experiment at hand.

Because of the very high gain of the log amplifier when its input is near $V = 0$ ($V < 1$ mV), care must be taken to balance the direct current (dc) level of all components and also to minimize the input noise. The effects of having a dc offset on the output of the voltage clamp are shown near the beginning of the results section (Fig. 4). To get useful log records at very low membrane currents, we used an analog filter (model 3322R; Krohn-Hite Corp., Avon, Mass.) in its low-pass (24 dB/octave) setting; generally, the filter was used at 10–40 Hz cutoff.

The direct and log-transformed voltage-clamp outputs were displayed on a storage oscilloscope, and each also drove one channel of a rectilinear chart recorded (model 220; Brush).

C. Computation

Eq. 6 was solved numerically on a PDP 11/45 computer (Digital Equipment Corp., Maynard, Mass.). Solutions were displayed on a Tektronix graphics terminal (Tektronix, Inc, Beaverton, Ohio), and produced in final form on a Calcomp incremental plotter (California Computer Products, Inc., Anaheim, Calif.).

We used the Adams-Bashforth "predictor-corrector" method (Kunz, 1957; chap. 9) to solve our differential equations. This procedure uses a variable integration increment whose size is adjusted according to the size of a calculated error parameter in such a way that the parameter is kept between preset limits. Allowing the step size to increase as the absolute value of the derivative (and therefore the error parameter) decreases makes the actual solution time small compared with methods that always use the small step size needed for accuracy where the solution is steep.

The only difficulty we encountered with this method occurred when we wanted to display a derivative rather than a solution. Because of the variable step size, the derivatives may appear lumpy, as in Figs. 2 and 3 of paper II. The obvious bumps on the rising and falling phases of the calculated gating current reflect the rapid shifts of the step size as the solution for the conductance itself becomes steep and then flattens out.

RESULTS

A. The Form of Individual Conductance Responses

In Fig. 1, we see the sorts of monazomycin-induced conductance changes we will analyze in detail. Fig. 1 *a* and *b* is, respectively, the linear and logarithmic

records of membrane current after a voltage step from $V = 0$ to $V = 60$ mV. As advertised above, the turn-on of conductance is S shaped. (Since the membrane voltage is constant for the whole record, records of current vs. time are simply scaled records of conductance vs. time.) The log record reveals, however, that the S has a particular character. The initial lag and part of the upswing comprise a domain in which the conductance is climbing exponentially. In other words, there is a period of time when the conductance is governed by the growth law (Eq. 1):

$$g = g_0 e^{At}, \tag{1}$$

where A is the rate constant of the rise ($A = 1/\tau$) and t is the time elapsed after the voltage switch. Equivalently, we may write

$$\ln \frac{g}{g_0} = At, \tag{2}$$

which conforms better to how we actually observe the system.

This growth characteristic of the early conductance rise allows us to associate a single number (A) with the speed of the early part of the turn-on. As we will see shortly, A varies in simple and interesting ways with transmembrane potential and monazomycin concentration.

Fig. 1 *c* and *d* are again linear and logarithmic, but in this case show the decay of conductance after a voltage step from $V = 50$ to 10 mV. The linear record might be interpreted as a first-order decay process of the form

$$g = g_0 e^{-At}, \tag{3}$$

but the logarithmic record, which would then be a straight line, belies this interpretation. In fact, the log I response cannot be described as the sum of two or three or any small number of first-order processes. Rather, it appears to be an exponential decay with a continuously slowing rate constant. We will shortly see that this statement is quantitatively accurate.

The *traces* in Fig. 1 are sufficient to prove that the monazomycin kinetics cannot be adequately fitted by the Hodgkin and Huxley (1952) scheme for the potassium system of squid giant axon, which is summarized by Eq. 4:

$$g = \{g_\infty^{1/N} - (g_\infty^{1/N} - g_0^{1/N})e^{-At}\}^N, \tag{4}$$

where g_0 is the initial conductance, g_∞ is the steady-state conductance reached after a long voltage step and N is an empirical parameter. Hodgkin and Huxley chose $N = 4$ as a compromise between ease of computation (which demands small N) and accuracy of fit to the experimental kinetic curves (which would require $N > 4$) (Hodgkin and Huxley, 1952; Eq. 11, p. 508, *et seq.*).

The inability of Eq. 4 to account for the monazomycin conductance decay is most easily seen by solving Eq. 4 for the rate constant A:

$$A = \frac{\ln(\{g_0^{1/N} - g_\infty^{1/N}\}/\{g^{1/N} - g_\infty^{1/N}\})}{t}. \tag{5}$$

We may now substitute measured values of g at various times after the voltage switch along with g_0 and g_∞ and see if A is actually a constant. In Fig.

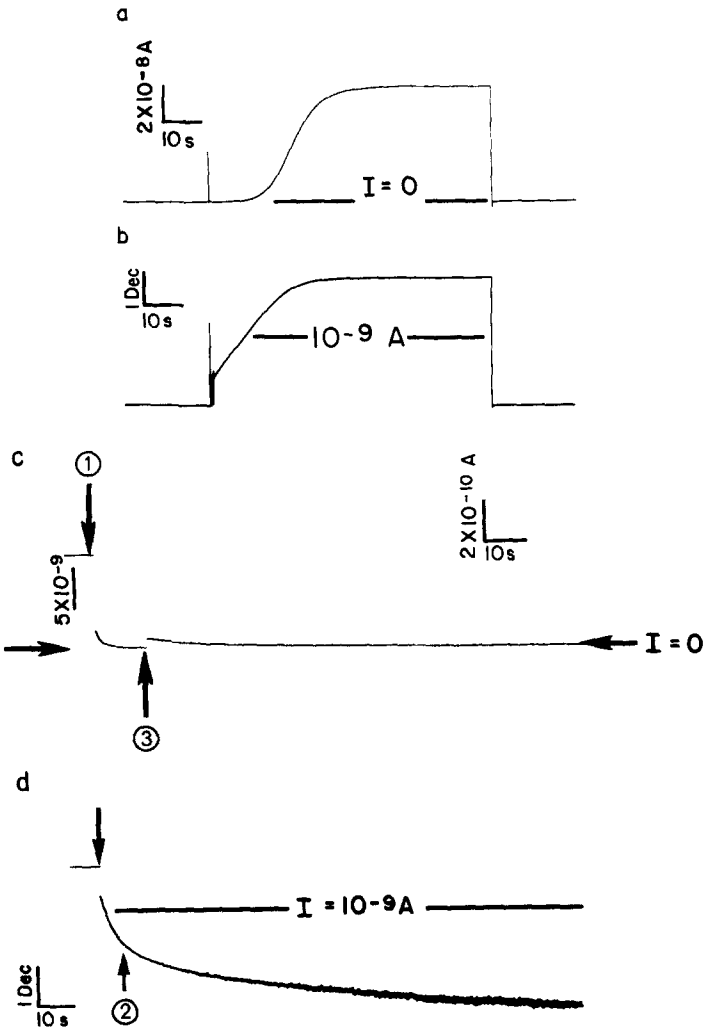

FIGURE 1. (*a*) And (*b*) are, respectively, the linear and logarithmic current increases in response to a step of voltage from $V = 0$ to $V = 60$ mV at the time indicated by the capacitance spikes; the return to $V = 0$ is signalled by the return of the linear current to zero. (*a*) Shows the usual S-shaped monazomycin conductance increase, and (*b*) reveals the underlying exponential nature of the early part of the "S." Solving Eq. 6 with $g_0 = 8 \times 10^{-10}\ \Omega^{-1}$, $g_\infty = 1.17 \times 10^{-6}\ \Omega^{-1}$, $A = 3.8 \times 10^{-1}\ s^{-1}$, and B = 0.7 will reproduce (*a*) or (*b*). The monazomycin concentration was $7.5 \times 10^{-7}\ g \cdot ml^{-1}$. The low-pass filter was set at 20 Hz. (*c*) And (*d*) are, respectively, the linear and logarithmic current decays in response to a voltage step from $V = 50$ to $V = 10$ mV at the time indicated by the *arrows* marked *1*. Note that the conductance just before and after the step is the same; the current is instantaneously proportional to *V*. At *arrow 2* the low-pass filter setting was changed from 100 to 10 Hz. The high initial level was necessary to prevent distortion of the fast transient at the time of the voltage step, and the lower cut-off was needed to minimize noise as *I* approached zero and the gain of the logarithmic amplifier increased; the increase of the noise in the logarithmic recording at low *I* is nevertheless evident. At *arrow 3*, the gain of

2, A is plotted against t for N = 4, 10, and 100. The continual decrease of A is evident; we conclude that Eq. 4 is not a good description of the monazomycin conductance decay. It is important to note that the decline of A is not an artifact of the value of g_∞, the residual conductance. The value of g_∞ used in the calculations for Fig. 2 was $2 \times 10^{-10}\ \Omega^{-1}$, as actually measured.[2] Raising g_∞ to 5×10^{-10} or lowering it to $5 \times 10^{-11}\ \Omega^{-1}$ (the value predicted at 10 mV by extrapolation from g_∞ at 50 mV using Eq. 14) does not alter our conclusion.

Similar arguments convince us that Eq. 4 is of the wrong form to generate the monazomycin turn-on kinetics (Fig. 1 *a* and *b*). No matter how small g_0 is made nor how much we increase N, numerical solutions show that log g visibly bends toward the time axis in much less than one decade of conductance rise. If we again use Eq. 5 on monazomycin data, we now find that the calculated value of A continually increases with time after the voltage step, regardless of the selected value of N (Fig. 3).

B. The dc Level of the System

Because much of our subsequent analysis of the data and our formal treatment rests on the finding that the initial conductance rise is exponential, we illustrate the effects of intentionally shifting the dc level of the voltage-clamp output on the form of the log I record in Fig. 4. In Fig. 4*a*, we adjusted the input to the log amplifier so that it was at +2.0 mV when $I = 0$. Because the log amplifier will not come out of saturation until its input is more negative[3] than about $-100\ \mu$V, log I will initially be indeterminate and will only assume its linear time-course once g gets sufficiently large.

In Fig. 4*b*, we produced an imbalance of −2.0 mV at the input to the log amplifier, which causes the log I response to take on an S shape. The initial horizontal part of the record merely reflects that the earliest current through the conductance will produce a voltage-clamp output considerably smaller than the offset. It is only when the output of the voltage clamp due to the actual current exceeds the potential offset by a factor of three or more that the exponential growth becomes evident. This same sort of record is obtained if the membrane has a relatively high leakage conductance.

Thus, the apparent nature of the log I response changes dramatically

[2] The leakage conductance of the unmodified membrane was $8 \times 10^{-11}\ \Omega^{-1}$. The voltage-independent conductance rose to $2 \times 10^{-10}\ \Omega^{-1}$ after the antibiotic addition. This parallel conductance is, we believe, due to the existence of monazomycin channels whose charges stay in the *cis* solution so that their number is unaffected by V. (Results, part *F*).

[3] The current-to-voltage converter of the voltage clamp is an inverting amplifier. Thus, increasing positive current is associated with an increasingly negative output.

---

the linear channel was increased 25-fold to make part of the long tail visible. Records (*c*) and (*d*) are truncated to save space. At the end of the truncated logarithmic tracing, I had declined to $\sim 3 \times 10^{-10}\ \Omega^{-1}$. The steady-state of $2 \times 10^{-10}\ \Omega^{-1}$ was reached ~90 s later. Solving Eq. 6 with $g_0 = 2.25 \times 10^{-7}\ \Omega^{-1}$, $g_\infty = 2 \times 10^{-10}\ \Omega^{-1}$, $A = 1.2\,8 \times 10^{-2}\ s^{-1}$ and B = 0.7 will reproduce (*c*) or (*d*). The monazomycin concentration was $2 \times 10^{-6}\ g \cdot ml^{-1}$.

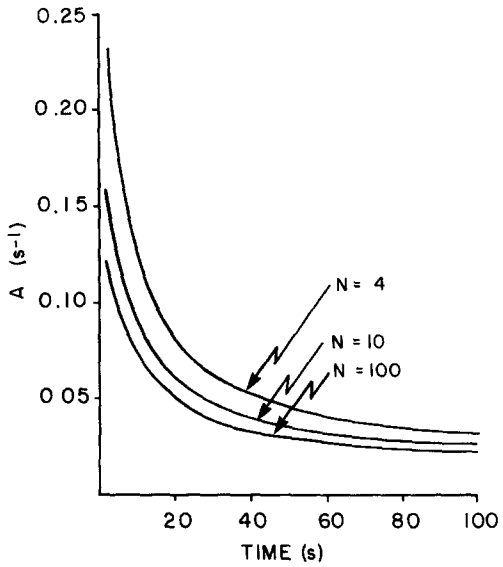

FIGURE 2. Variation of the rate "constant" A, as defined by the Hodgkin and Huxley (1952) potassium kinetic equation (Eq. 5), during the monazomycin conductance decrease of Fig. 1 *c* and *d*. Values of N = 4, 10, and 100 are shown. Making N even larger produced little further change in the position of the curve. $g_0 = 2.3 \times 10^{-7}\ \Omega^{-1}$, $g_\infty = 2 \times 10^{-10}\ \Omega^{-1}$. The variation of A with time occurs even if higher or lower values of g_∞ are chosen (see text).

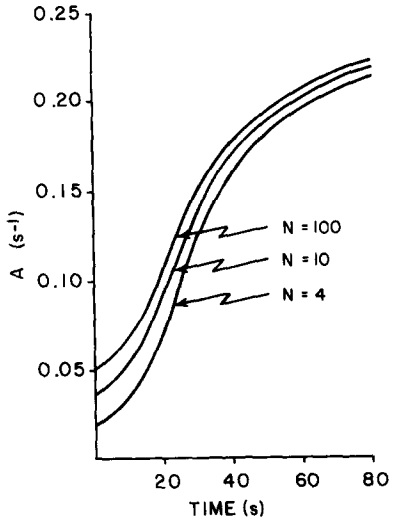

FIGURE 3. Variation of the rate "constant" A, as defined by the Hodgkin and Huxley (1952) potassium kinetic equation (Eq. 5), during the monazomycin conductance increase of Fig. 1 *a* and *b*. Values of N = 4, 10, and 100 are shown. Making N even larger did not change the shape of the curve very much. $g_0 = 8 \times 10^{-10}\ \Omega^{-1}$, $g_\infty = 1.17 \times 10^{-6}\ \Omega^{-1}$.

around the proper dc level of the voltage clamp. In fact, this characteristic of the systems is so sensitive that it is possible to zero the current-to-voltage converter to within 100 μV by adjusting its offset potentiometer until the beginning of the log I response becomes linear. We take this as evidence that the initial exponential current rise reflects the true behavior of the conductance.

C. An Empirical Rate Equation for the Kinetics

We find that numerical solutions of Eq. 6 can be superimposed on both linear and logarithmic current vs. time records; the adequacy of the fit is demonstrated in Fig. 5.

$$\frac{dg}{dt} = Ag\left[1 - \left(\frac{g}{g_\infty}\right)^B\right]. \tag{6}$$

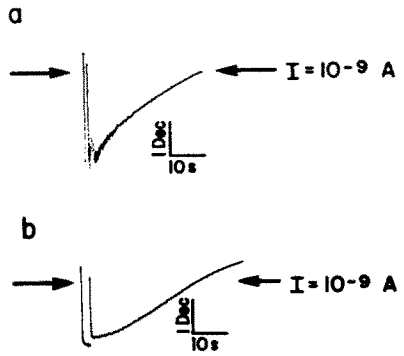

FIGURE 4. The effects of intentionally offsetting the dc level of the input to the logarithmic amplifier (*a*) +2.0-mV offset; (*b*) −2.0-mV offset. Further description in text. (*a*) And (*b*) are in response to a step from $V = 0$ to $V = 50$ mV; in both cases the membrane potential was held at $V = -100$ mV, and set to 0 mV for ~2 s before the step. The monazomycin concentration was 2.0×10^{-6} g·ml^{-1}.

A is the slope of the linear portion in the log I records, whereas B for now can be taken as a positive parameter whose value can be determined by varying it until the best match between the experimental and computed curves is obtained. B is numerically equal to ~0.7; we have not found it necessary to vary it for any of the data analyzed. As we will see in paper II, the value of B should depend only on the molecularity of aqueous, oligomeric monazomycin aggregates that enter and leave the membrane and on the molecularity of the channels themselves. It is thus gratifying that B is essentially constant over a wide range of g_∞, V, and [Mon]. A, on the other hand, is a strong function of all three of the just-cited variables.

That Eq. 6 is at least a reasonable form for the monazomycin conductance

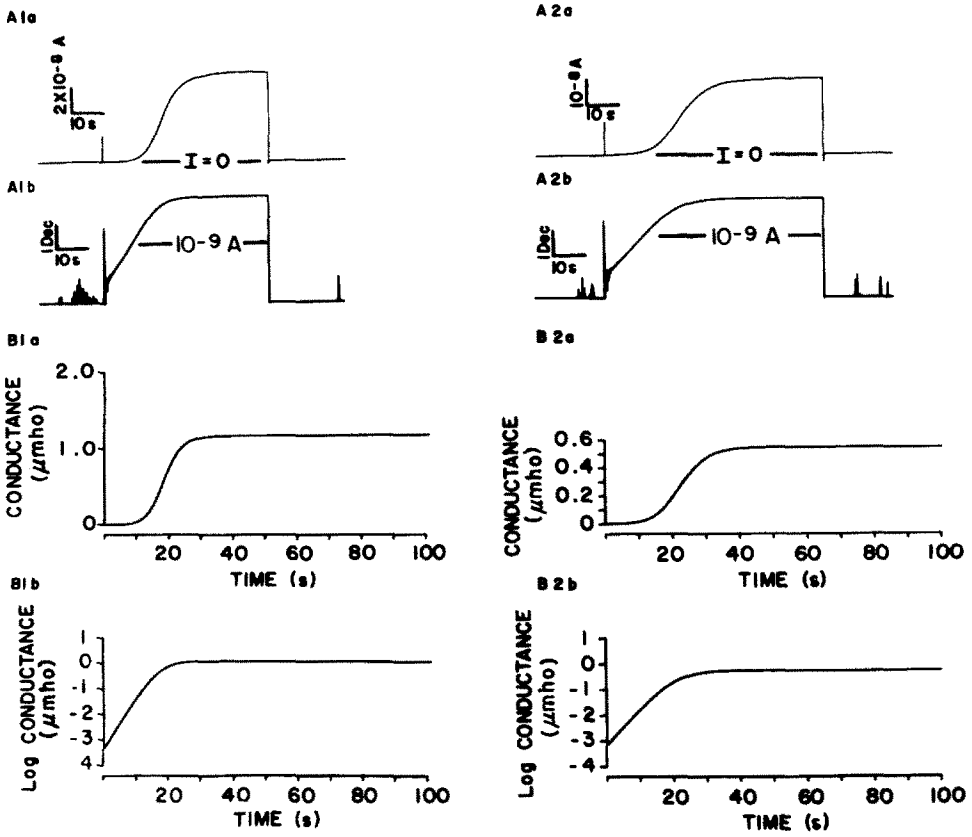

FIGURE 5. Demonstration of the ability of solutions of Eq. 6 to reproduce monazomycin conductance increases. Calculated curves have been scaled to be the same size as the corresponding experimental responses, so that the accuracy of the fits may be checked using tracing paper. Note that the gain (or scale, in the calculated curves) is the same for all logarithmic records, whereas the gain of the linear records varies. (*A*) Experimental records. *A 1–3* are three successive responses from the same film after steps from $V = 0$ to $V = 60$ mV (*A* 1), $V = 55$ mV (*A* 2) and $V = 50$ mV (*A 3*). The membrane potential was held at -100 mV for 1 min and then set to $V = 0$ for 15 s before each step. (*a*) And (*b*) for parts *A 1–3* are linear and logarithmic traces, respectively. The monazomycin concentration was 7.5×10^{-7} g·ml^{-1}. (*B*) Calculated responses using Eq. 6. *B 1–3* correspond to *A 1–3*; (*a*) and (*b*) of each part are on linear and logarithmic scales. The solution parameters were: *A 1*: $g_0 = 4.3 \times 10^{-10}\ \Omega^{-1}$, $g_\infty = 1.17 \times 10^{-6}\ \Omega^{-1}$, $A = 4.64 \times 10^{-1}$ s, *A 2*: $g_0 = 7.0 \times 10^{-10}\ \Omega^{-1}$, $g_\infty = 5.42 \times 10^{-7}\ \Omega^{-1}$, $A = 3.22 \times 10^{-1}$ s^{-1}. *A 3*: $g_0 = 5.0 \times 10^{-10}\ \Omega^{-1}$, $g_\infty = 2.30 \times 10^{-7}\ \Omega^{-1}$, $A = 2.15 \times 10^{-1}$ s^{-1}. In all cases, B = 0.7. Note that the calculated responses are given as conductances. The linear plots are sized to fit directly on the experimental records; only the scales are different. For the logarithmic plots, the size of one decade was preserved, with the result that the calculated curve is displaced along the logarithmic axis by a factor equal to the logarithmic of the applied potential. Because the potentials are all very similar, the displacement corresponds to ~1.25 decades for each.

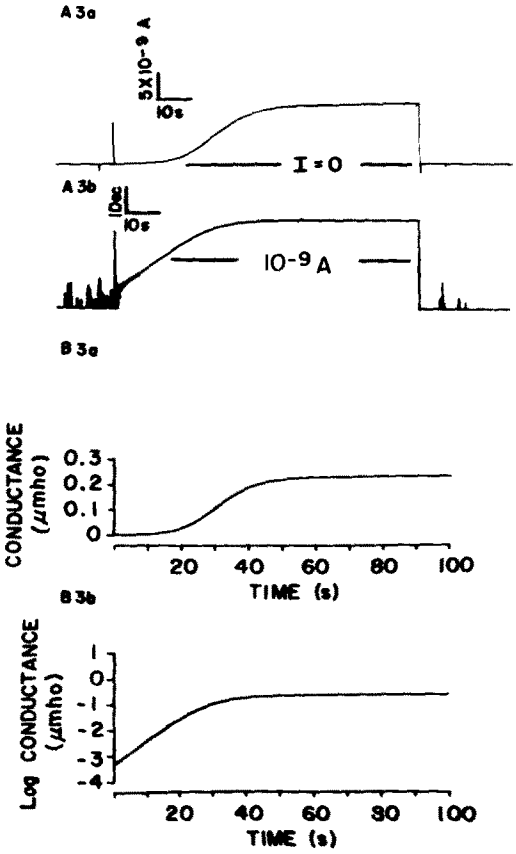

FIGURE 5

can be seen by considering extreme cases. For a conductance increase, we take $\frac{g}{g_\infty} \ll 1$ for short times after the positive voltage step. Then Eq. 6 is approximated by:

$$\frac{dg}{dt} = Ag, \tag{7}$$

which is the proper form to yield the initial exponential increase. Of course, as $g \rightarrow g_\infty$, the time derivative of the conductance will go to zero. How quickly this happens is a function of the value of B. For large values of B, $\left(\frac{g}{g_\infty}\right)^B$ will remain very small until $g \approx g_\infty$. Thus, large values of B will generate solutions that remain nearly exponential until the steady state is reached. For small values of B, the magnitude of dg/dt will very quickly fall below the exponential and it will therefore take a great deal of time for the conductance to become nearly constant. We illustrate the effects of varying B in Fig. 6; the curve with $B = 0.7$ represents the actual behavior of the conductance.

For conductance decreases, $\frac{g}{g_\infty} \gg 1$ at the outset. Shortly after a negative voltage step, Eq. 6 then behaves as:

$$\frac{dg}{dt} = -Ag\left(\frac{g}{g_\infty}\right)^B. \tag{8}$$

If we take $\left(\frac{g}{g_\infty}\right)^B$ to be a constant, Eq. 8 integrates to:

$$g = g_0 e^{-A\left(\frac{g}{g_\infty}\right)^B t}. \tag{9}$$

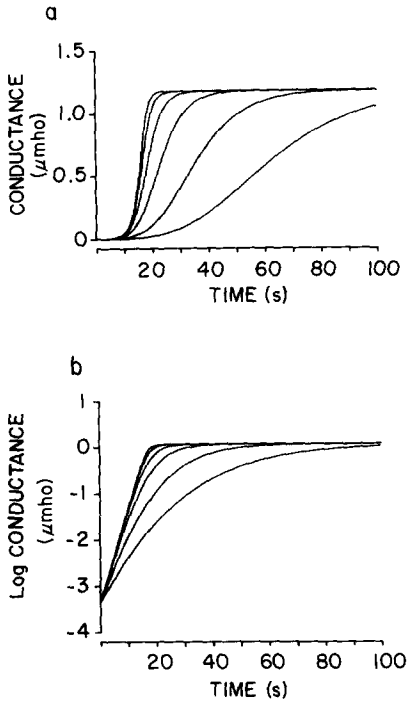

FIGURE 6. The effect of varying B in Eq. 6 on the shape of the solution for a conductance increase. The other parameters, $g_0 = 4.3 \times 10^{-10}$ Ω^{-1}, $g_\infty = 1.17 \times 10^{-6}$ Ω^{-1} and $A = 4.64 \times 10^{-1}$ s^{-1}, are taken from the response in Fig. 5, parts *A l a* and *A l b*. (*a*) Is linear, (*b*) is logarithmic. Starting with the curves in (*a*) and (*b*) which remain closer to the time axis longer, the values of B are 0.1, 0.2, 0.4, 0.7, 1.2, and 1.8.

Thus, we have an exponential conductance decay with a continuously decreasing rate constant, in accordance with observation. In Fig. 7, we show how changing B will affect the time-course of the decay. It is obvious that the initial part of the fall is very sensitive to changing B. Note, however, that as $g \rightarrow g_\infty$, Eq. 6 again requires the derivative to go to zero.

Eq. 6 may be directly integrated to give

$$g = \frac{g_0 e^{At}}{\left[1 + \left(\frac{g_0}{g_\infty}\right)^B (e^{ABt} - 1)\right]^{1/B}}. \tag{10}$$

D. Numerical Solutions of the Rate Equation

1. CONDUCTANCE INCREASES The easiest responses to match with a solution of Eq. 6 are those where the steady-state conductance is three orders of magnitude or more greater than the initial conductance. In such cases, the growth process is seen in isolation for a long enough time that the value of A may be read directly from the log I vs. t record. In practice, we determine the time required for g to increase one decade (t_{dec}) and get A from

$$A = \frac{\ln 10}{t_{dec}} \tag{11}$$

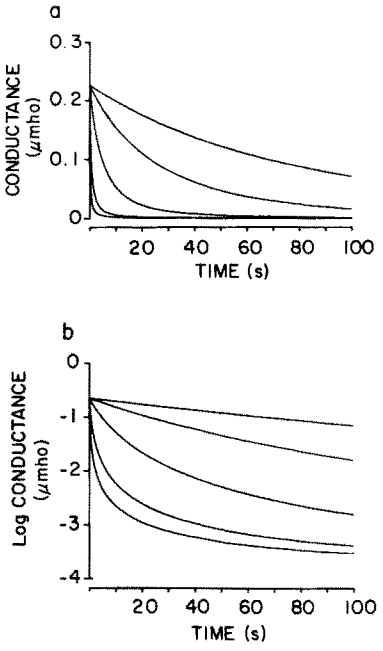

FIGURE 7. The effect of varying B in Eq. 6 on the shape of the solution for a conductance decrease. The other parameters, $2.25 \times 10^{-7}\ \Omega^{-1}$, $g_\infty = 2.0 \times 10^{-10}\ \Omega^{-1}$ and $A = 1.28 \times 10^{-2}$, are taken from the response of Fig. 1 (*c*) and (*d*). (*a*) Is linear, (*b*) is logarithmic. Starting with the curves in (*a*) and (*b*) which approach the time axis most rapidly, the values of B are 0.9, 0.7, 0.4, 0.2, and 0.1.

The value of g_0 is more problematical. Most of our experiments were done under conditions where it was impractical to measure g_0 directly because the holding potential was low enough to make g_0 comparable to the leakage conductance of the unmodified membrane. (In other words, our voltage steps began when only a very few monazomycin channels were conducting.) Thus, for the most part, we obtained g_0 by extrapolating the linear part of the log I vs. V record to $t = 0$. This is not a very accurate procedure because of the logarithmic scale; errors of 10 or 20% are to be expected. Nevertheless, the solutions of Eq. 6 are not materially affected. Because the gain of the linear channel is chosen to make I equal to or less than a full-scale deflection, changing g_0 will merely shorten or prolong the initial horizontal portion

during which I appears to stay at zero. Similarly, varying g_0 will only lengthen or reduce the linear region of the log I record. The effects of altering g_0 are shown in Fig. 8. The validity of this extrapolation procedure was proved by making voltage steps from levels where g_0 was high enough to be directly measured. No problems were encountered even though the value of A was harder to obtain.

In a few instances, we solved Eq. 6 for responses that had no obvious growth region because g_∞ was not high enough. Two methods were used to get A. First, we treated A as a parameter to get the best fit. Values gotten in this way

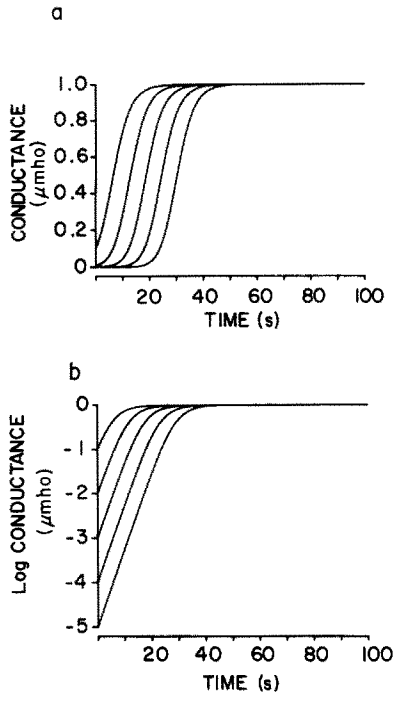

FIGURE 8. The effect of varying g_0 in Eq. 6 on the shape of the solution for a conductance increase. $g_\infty = 1.0 \times 10^{-6}\ \Omega^{-1}$, $A = 4.0 \times 10^{-1}\ s^{-1}$, B = 0.7. Starting with the solution that has the longest initial horizontal limb (*a*, linear) or reaches the steady-state last (*b*, logarithmic) the values of g_0 are 1×10^{-11}, 1×10^{-10}, 1×10^{-9}, 1×10^{-8}, and $1 \times 10^{-7}\ \Omega^{-1}$.

were in good agreement with those obtained by extrapolating the function connecting A and V (Results, part *E*) to the potential applied during the step.

2. CONDUCTANCE DECREASES Although A is initially defined from the shape of conductance increases, it should be only a function of the membrane potential and not the history of stimulation.[4] We find this is indeed the case for conductance decreases to levels high enough that the value of A could be

[4] Assuming fixed monazomycin concentration, etc. This is not a theoretical point. The *inset* in Fig. 9 shows the log current as V is switched from 60 to 70 to 80 mV. We see that the slope of log I changes as soon as the voltage is changed.

directly determined from previous conductance increases. Even though the decrease shown in Fig. 9*a* after a step from 80 to 70 mV is qualitatively different than the increase of Fig. 9*b* after a step from 0 mV to 70 mV, A must be the same for Eq. 6 to generate adequate reproductions.

For conductance decreases to steady states below the range that allows us to find A directly, we can again treat A as a parameter; as described above, extrapolation from the A vs. V function to the applied potential gives a similar answer.

3. INTERACTIONS BETWEEN THE CONSTANTS A AND B. It is possible to simultaneously vary A and B in Eq. 6 in such a way that the solution, when plotted as a linear I vs. t curve, appears to remain invariant.

Specifically, if we choose too low a value for A, we can compensate by increasing B. This trade-off is possible because the exponential nature of the early conductance rise is not visible in the linear record. Accordingly, if A is intentionally made too small, increasing B will let the solution adhere closer to the exponential for a longer period of time, and will therefore steepen the major segment of the rise sufficiently. This error is precluded if we make the solution fit the log I vs. t record as well as the linear one.

To summarize, we believe Eq. 6 is adequate to describe conductance changes after voltage steps. Although it is true that there are circumstances under which the behavior of the conductance is more complex than predicted (see below and paper II), any complete theory for monazomycin kinetics will have to include Eq. 6 as a widely applicable limiting form. We now turn to the question of how the rate constant A is determined by the physical state of the system.

E. The Dependence of the Rate Constant on the Membrane Potential.

In Fig. 10, we show how A (Fig. 10*a*) and g_∞ (Fig. 10*b*) vary when voltage steps from $V = 0$ to various levels are made. Between each pair of measurements, the membrane potential was set to $V = -100$ mV for 1.0 min to ensure the state of the membrane was the same before each step.

The relationship between g_∞ and V is (Muller and Finkelstein, 1972*a*):

$$g_\infty = g_* e^{nqV/kT}, \tag{12}$$

where g_* is g_∞ at $V = 0$, q is the electronic change, k is Boltzmann's constant, T is the absolute temperature; and n is the slope of the log g_∞ vs. V line at fixed temperature and is numerically equal to ~5.2 (Table I).

Interestingly, the dependence of A on V has the same form, differing only by the smaller slope:

$$A = A_* e^{yqV/kT}, \tag{13}$$

where y is numerically equal to ~2.4 (Table I). Given Eqs. 12 and 13, it is not surprising that a plot of log A vs. log g_∞ yields a straight line of slope y/n (Fig. 10*c*).

It is evident that Eqs. 12 and 13 must fail if we attempt to use too large a

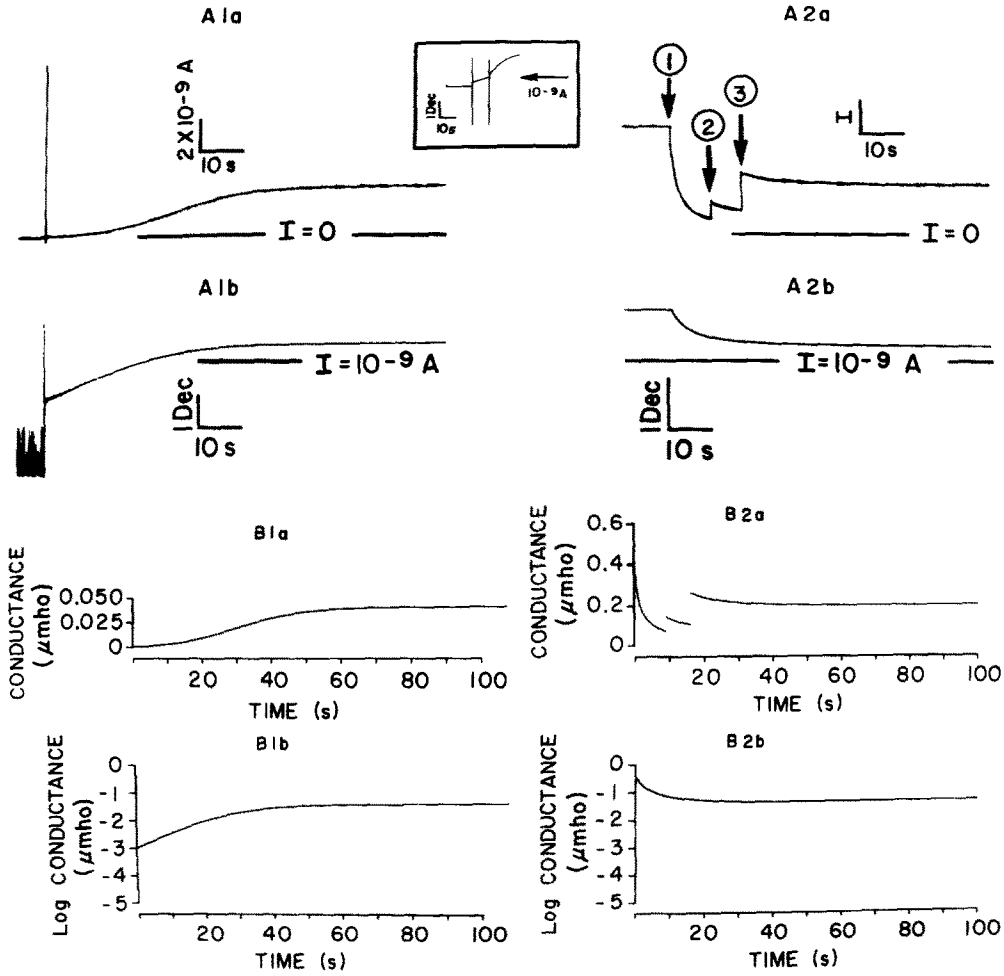

FIGURE 9. *A 1* shows a conductance increase after a step from $V = 0$ to $V = 70$ mV. *A 2* is a conductance decrease after a step from $V = 80$ to $V = 70$ mV, taken ~5 min after *A 1*. Note that the steady-state current is the same in both cases. For *A 1* and *A 2* parts (*a*) and (*b*) are, respectively, linear and logarithmic recordings. The monazomycin concentration was 1.0×10^{-6} g·ml^{-1}. The low-pass filter was set at 30 Hz. *B 1* shows linear (*a*) and logarithmic (*b*) plots of a solution of Eq. 6 which superimpose on the corresponding parts of *A 1*. The solution parameters were $g_0 = 1.01 \times 10^{-9}\ \Omega^{-1}$, $g_\infty = 4.09 \times 10^{-8}\ \Omega^{-1}$, $A = 1.38 \times 10^{-1}\ s^{-1}$ and B = 0.7 (*B 2*) shows linear (*a*) and logarithmic (*b*) plots of a solution of Eq. 6 which superimpose on the corresponding parts of *A 2*. The solution parameters were $g_\infty = 4.0 \times 10^{-8}\ \Omega^{-1}$, $A = 1.38 \times 10^{-1}\ s^{-1}$ and B = 0.7. *B 2a* was produced by scaling the same solution three times to match the gain changes in *A 2a*. (From the beginning of the record to *arrow 1*, the current calibration bar represents 10^{-8} A, between *arrows 2* and *3*, 5×10^{-9} A and after *arrow 3*, 2×10^{-9} A.) Only the relevant parts of the three reproductions are shown; the scale in *B 2a* applies to the lowest gain only. As in Fig. 5, the

voltage range. Eq. 12 holds quite well down to at least 10^{-10} Ω^{-1} when correction for the leakage conductance is made. At extremely low levels, the strength of the voltage dependence weakens (Muller and Andersen, manuscript in preparation; see also Results, part *F*). On the high end, Eq. 12 is good to $\sim 10^{-4}$ Ω^{-1} (Heyer et al., 1976). Mueller (1979) reports that the conductance ultimately becomes voltage independent when it reaches a level of $\sim 1.5 \times 10^{-4}$ Ω^{-1} (normalizing to our membrane area) using uncharged lecithin bilayers in 0.1 M salt. For our charged PG films this would correspond to a maximum conductance of a few times 10^{-3} Ω^{-1}.

We did not investigate this saturation of the conductance, because we used a two-electrode voltage clamp and would have had to make enormous corrections for the series-access resistance. It was, however, possible to see how A behaved in response to potentials that presumably would have generated very high steady conductances simply by looking at the log I record at short times. The initial parts of the records were still linear, but the dependence of A on V became much weaker (Fig. 11). We have not systematically investigated how the decreased dependence of A on V varied with monazomycin conductance.

F. Dependence of the Rate Constant on Monazomycin Concentration

Fig. 12 summarizes the outcome of an experiment in which A and g were measured for several potential steps from $V = 0$ mV at each of four monazomycin concentrations; again, the potential was held at -100 mV for 1 min between positive steps.

The value of g_∞ (Fig. 12*b*) is given by:

$$g_\infty = g_* \left(\frac{[\text{Mon}]}{[\text{Mon}]_*}\right)^s e^{nqV/kT}, \tag{14}$$

where now g_* is the value of g_∞ at $V = 0$ mV with $[\text{Mon}] = [\text{Mon}]_*$; s is a constant equal to 5.76 (Table I). Because each concentration change is a doubling, Eq. 14 predicts that the successive shifts along the voltage axis should be of equal size. In fact, the first doubling leads to a bigger shift than the others. We agree with Mueller (1979) that the concentration dependence of g_∞ is usually greater at low monazomycin concentration. Associated with this feature is a somewhat weaker voltage dependence (Fig. 12).

Evidently, from the data of Fig. 12*a*, the value of A can be described by an

---

calculated responses are presented as conductances. The displacement in the logarithmic records is 1.15 decades. *Inset*: The logarithmic trace shows the effect of going from the steady-state at 60–70 mV for 10 s and then to 80 mV. Within experimental error (i.e., time resolution) the rate constant A immediately assumes the value characteristic for the applied potential. The monazomycin concentration was 1×10^{-6} g·ml^{-1}. The low-pass filter was set at 20 Hz.

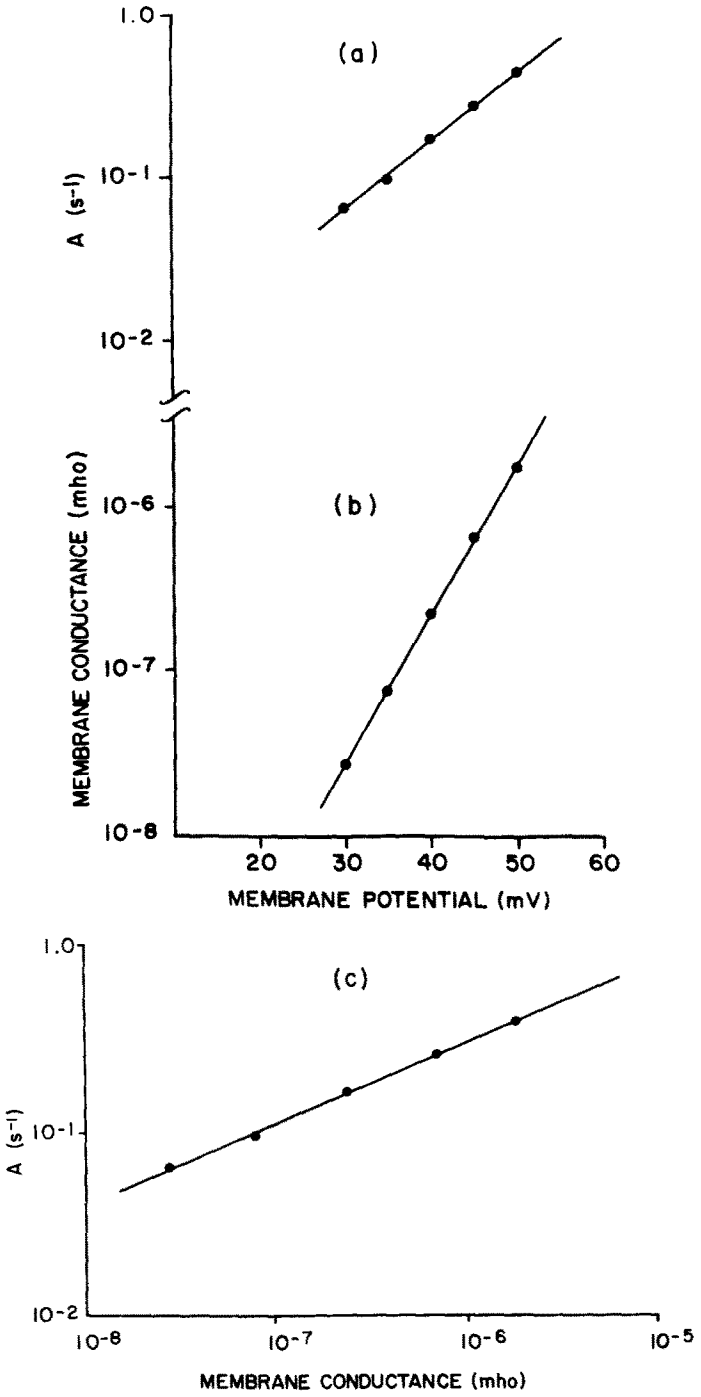

FIGURE 10. (*a*) The dependence of the rate constant A on membrane potential. Given the logarithmic axis for A, the relationship is seen to be exponential, such

equation of the same form as Eq. 14:

$$A = A_*\left(\frac{[\text{Mon}]}{[\text{Mon}]_*}\right)^{\text{x}} e^{yqV/kT}, \tag{15}$$

where x is a fourth constant equal to 2.63 (Table I).

In Fig. 12*c*, we plot log A vs. log g_∞ using a different symbol for the A-g_∞ points for each concentration. Only two lines are drawn because the points from the three highest monazomycin concentrations are colinear within experimental error. The shifted log A-log g_∞ characteristic at low concentration reflects the deviation of A and g_∞ from the simple relationships of Eq. 14 and 15 described above. The meaning of a displacement is most easily seen by

TABLE I

AVERAGED VALUES FOR THE FOUR PARAMETERS IN Eq. 18

	Parameter			
	Conductance		Kinetics	
	s	n	x	y
Mean value	5.76	5.20	2.63	2.39
SD	0.77	0.50	0.73	0.26
Number of measurements	17	32	17	32
$\left(\frac{\text{x}}{\text{s}}\right) = 0.457$		$\left(\frac{\text{y}}{\text{n}}\right) = 0.460$		

The coefficient of correlation (17 pairs) between the concentration-dependent parameters x and s is $r = 0.75$; that for the voltage-dependent parameters (32 pairs) is $r = 0.56$. The probability of either value of r occurring by chance is $P < 0.001$. The Student's t test value for the difference of the means of s and n is 3.17 ($P < 0.003$); that for the difference of the means of x and y is 1.74 ($P < 0.09$).

writing the equation of a log A-log g_∞ line:

$$\ln\left(\frac{A}{A_*}\right) = \frac{\text{y}}{\text{n}}\ln\left(\frac{g}{g_*}\right) + \left(\text{x} - \frac{\text{sy}}{\text{n}}\right)\ln\left(\frac{[\text{Mon}]}{[\text{Mon}]_*}\right). \tag{16}$$

Colinearity of points in spite of changing [Mon] thus requires:

$$\text{x} - \frac{\text{sy}}{\text{n}} = 0. \tag{17}$$

---

that a 10.4-mV change of potential generates an e-fold change of A (i.e., y = 2.45). (*b*) The dependence of g_∞ on membrane potential. A 4.8-mV change of potential causes an e-fold change of g (n = 5.36). (*c*) Log A as a function of log g_∞. A and g_∞ pairs are taken from individual conductance increases. The slope of the line is y/n = 0.46. The monazomycin concentration was 5.0×10^{-6} g·ml^{-1}.

From Table I, we see this is numerically almost exactly true for averaged values of the four parameters ($x - sy/n = 0.017$).

That Eq. 17 holds may at first glance appear fortuitous, but from another point of view it is almost required. Parameters s and n measure, respectively, the concentration and voltage dependence of an oligomeric monazomycin species, namely, the channels. Each may be regarded as an estimate of the molecularity of that species. Thus, s/n describes the relative effectiveness of chemical and electrical energy in shifting the univalent monazomycin molecules into the membrane where they can participate in channel formation.

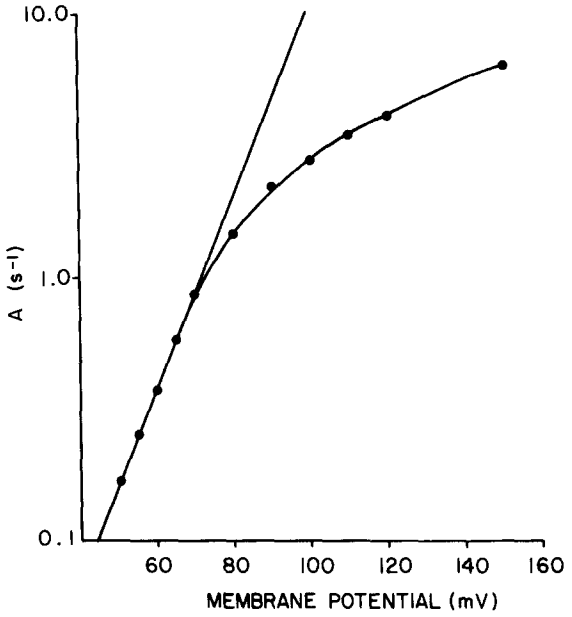

FIGURE 11. The decrease of the voltage-dependence of the rate constant A at high potential. For the line that passes through the five points from $V = 50$ to $V = 70$ mV, the value of y is 2.14. The (averaged) value of y between $V = 120$ and $V = 150$ mV is 0.37. The monazomycin concentration was 7.5×10^{-7} g·ml^{-1}.

From the form of Eq. 15, we can, by analogy, think of A as being proportional to the concentration of a smaller monazomycin aggregate. Thus, x/y again describes the relative effectiveness of chemical and electrical energy in moving monazomycin monomers. That $x/s = y/n$ is therefore a reasonable outcome theoretically and experimentally.

The closeness of the numerical values of n and s on the one hand and of x and y on the other, together with the rather large standard deviations (Table I), might be taken to mean that the dependencies of A and g_∞ on V and [Mon] are equal. We feel, however, that the inequalities $n \neq s$ and $y \neq x$ are real. A simple statistical calculation (Table I) reveals that it is very improbable that

the difference between n and s is a chance outcome. The difference between y and x is less dramatic, but it is in the same direction as the first. The weaker dependence of A and g_∞ on the membrane potential might be taken to mean that the positive charges of the monazomycin have not crossed the entire membrane thickness when they are in position to aggregate. Imagining a linear voltage gradient in the membrane allows the fraction of membrane thickness crossed by the charge (δ) to be calculated, in this case as:

$$\delta = \frac{n}{s} = \frac{y}{x} \approx 0.91.$$

This interpretation is, however, not attractive as an explanation in the monazomycin system. If the monazomycin charge lay this far into the membrane, it would feel a fair fraction of the dipolar voltage jump near the membrane-solution interface. The observation that steady-state monazomycin conductance is essentially unaffected by phloretin additions (*cis* and/or *trans*), which make the inner potential less positive, means that the monazomycin charge must move completely through the membrane, and therefore should feel the entire imposed potential difference (Andersen et al., 1976).

An alternative explanation of the weaker voltage dependence arises from an experiment in which enough monazomycin is added to the *cis* solution to generate a significant conductance at $V = 0$ mV. If we now add the same concentration to the *trans* solution, the conductance only doubles. We conclude that two independent, oppositely oriented channel populations can coexist in the membrane, for if oppositely oriented monomers could indiscriminately aggregate as channels, the *trans* addition would have caused a 2^8-fold conductance increase at $V = 0$ mV (Muller and Finkelstein, 1972*a*).

If we now suppose that monomers of one orientation are not absolutely excluded from contributing to oligomers which are mainly composed of oppositely oriented monomers, our problem is nearly solved. We add the supposition that when monazomycin is only in the *cis* solution, a small number of "wrong-way"-oriented molecules will get into the membrane. Such molecules of course have their positive charges sitting in the *cis* solution, so that their contribution depends only on monazomycin in concentration and not on V.[5]

We are now in a position to expand our empirical equation (Eq. 6) to include the dependence of A and g_∞ on monazomycin concentration and membrane potential using Eqs. 14 and 15:

$$\frac{dg}{dt} = A_* \left(\frac{[\text{Mon}]}{[\text{Mon}]_*}\right)^x e^{yqV/kT} g \left(1 - \left\{\frac{g}{g_* \left(\frac{[\text{Mon}]}{[\text{Mon}]_*}\right)^s e^{nqV/kT}}\right\}^B\right). \quad (18)$$

[5] The observation that sufficiently negative potentials can shut off the conductance indicates that the membrane concentration of "wrong-way" monazomycin must be very low with the aqueous concentrations ordinarily used. That such "wrong-way" molecules exist is shown by the development of voltage-independent conductance with very high monazomycin concentrations.

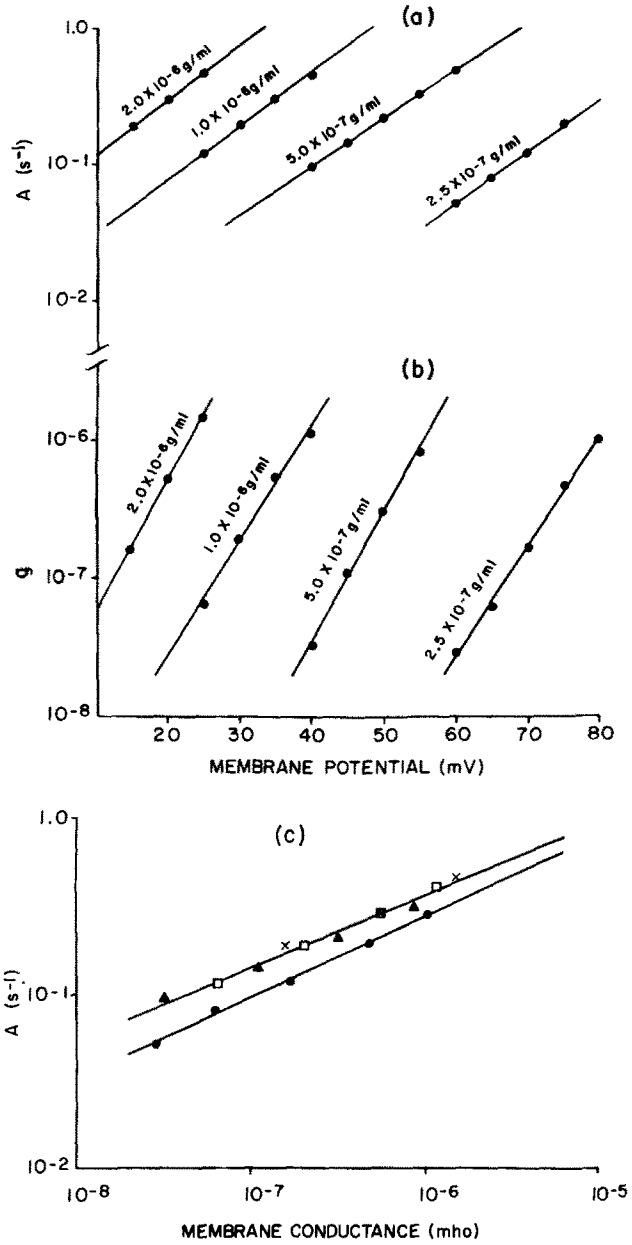

FIGURE 12. (*a*) Dependence of the log *A-V* characteristic on monazomycin concentration. The four lines were obtained with sequential monazomycin additions using one film; each line is labeled by the appropriate monazomycin concentration. The values of y (the voltage-dependent parameter for *A*), starting with the lowest monazomycin concentration are: 2.23, 2.08, 2.19, 2.31. The values of x (the concentration-dependent parameter for *A*), starting with the shift upon going from 2.5×10^{-7} g·ml^{-1} to 5.0×10^{-7} g·ml^{-1}, are: 3.21, 2.22,

If we expand in the parentheses, we get

$$\frac{dg}{dt} = A_* g \left(\frac{[\text{Mon}]}{[\text{Mon}]_*}\right)^x e^{yqV/kT} - A_* \left(\frac{[\text{Mon}]}{[\text{Mon}]_*}\right)^{x - sB} e^{(y - nB)qV/kT} g\left(\frac{g}{g_*}\right)^B. \quad (19)$$

Note that if $\left(\frac{x}{s} = \frac{y}{n}\right) = B$, Eq. 19 reduces to a very simple form:

$$\frac{dg}{dt} = A_* \left(\frac{[\text{Mon}]}{[\text{Mon}]_*}\right)^x e^{yqV/kt} g \left(1 - \left\{\frac{g}{g_*}\right\}^{x/s}\right). \quad (20)$$

Eq. 18 allows us in principle to calcualte how g varies in time in response to any sequence of applied potentials or to describe how the membrane potential would vary if we stimulated with constant current instead of a constant voltage. Eq. 20, which is quantitatively incorrect (because $x/s \neq B$) is the outcome of the first model we present in paper II. Eq. 19 arises from the somewhat more complicated second model in paper II.

G. Shifts of the Log A-Log g_∞ Characteristic

Any manipulation that affects only the conductance per channel would be expected to produce a parallel shift of the log A-log g_∞ along the conductance axis by an amount equal to the ratio of initial and final values. We observe this to be the case for a replication of an experiment done by Heyer et al. (1976). The membrane is initially bathed by symmetrical 0.1 M tetraethylammonium chloride (TEA). Qualitatively, the system was unchanged in that the initial part of the conductance was still exponential. Quantitatively, however, the log A-log g_∞ line was found further to the left than was ever seen in 0.1 M KCl. A subsequent *cis* and *trans* addition of 0.01 M KCl shifted the characteristic to the right. At constant A, the KCl addition caused a 4.2-fold change of g_∞ . Taking into account the 10-fold-lower K^+ concentration, K^+ is found to be ~42 times more permeant than TEA^+, in good agreement with the factor of 37 reported by Heyer et al. (1976).

A few experiments done on (relatively) uncharged PE + cholesterol membranes (2.5% PE + 1% cholesterol) bathed by 0.1 M KCl also yielded log A-

---

1.97. (*b*) Dependence of the log g_∞-V characteristic on monazomycin concentration; the same conductance increases as in (*a*) were measured. The values of n (the voltage-dependent parameter for g_∞), starting with the lowest monazomycin concentration, are: 4.65, 5.46, 4.95, 5.62. The values of s (the concentration-dependent parameter for g_∞) starting with the shift upon going from 2.5×10^{-7} g·ml^{-1} to $5.0 .\times 10^{-7}$ g·ml^{-1}, are: 6.35, 5.00, 4.52. (*c*) Log A as a function of log g_∞. The *line* with the solid dots (slope = 0.48) is for the lowest monazomycin concentration (2.5×10^{-7} g·ml^{-1}). The *upper line* is for 5.0×10^{-7} g·ml^{-1} (triangles), 1.0×10^{-6} g·ml^{-1} (squares) and 2.0×10^{-6} g·ml^{-1} (crosses).

log g_∞ characteristics outside the range seen with the PG-cholesterol films. Assuming that the shift to lower g_∞ at fixed A arose only from a lower interfacial K^+ for the PE film leads to reasonable values for the surface-charge density of the PE membranes $\sigma = 5 \times 10^{12}\ q\ cm^{-2}$ vs. $\sigma = 2 \times 10^{14}\ q\ cm^{-2}$ for the PG films (Muller and Finkelstein, 1972*b*).

A third kind of experiment along these lines gave surprising results. Addition of divalent cation to the *cis* solution will make the *cis* surface potential of a PG film less negative; this should affect g in three ways (Muller and Finkelstein, 1972*b*). First, the induced difference between the *cis* and *trans* surface potentials is in the direction to increase g_∞ . Second, the interfacial monazomycin concentration will decrease because monazomycin is a (univalent) cation. If s = n, these effects would cancel. In the actual case, because s > n, we expect g_∞ to decrease by about threefold after adding 0.03 M $MgCl_2$. Finally, the conductance per channel should decrease due to the reduced K^+ concentration at the *cis* interface. This effect should be nearly linear with the reduction of K^+ concentration, because we measured conductances at fairly high ($V \approx 100$ mV) positive potentials. On this basis alone, we expected g_∞ to drop by a factor of 12. The observed decrease of g_∞ at constant V was 28-fold, in good agreement with the prediction of a factor of 36. In spite of this, no shift was observed in the log A-log g_∞ line. We are forced to conclude that the Mg^{++} addition had some direct action on A; the basis of this result remains an open question.

H. Dependence of the Kinetics on the History of Stimulation

Fig. 13 illustrates an experiment in which steps from $V = 0$ to $V = 30$ mV are made from different initial conductances. (This is the same protocol we will use to demonstrate the memory in the accompanying paper.) Eq. 18 predicts that the conductance trajectory should be the same no matter how we reach a certain level at any given voltage. In other words, if the conductance starts at a relatively high level and proceeds to the steady-state, the time-course should superimpose on the relevant part of another response which starts at a lower level.

We see just this sort of behavior if the initial conductance is fairly low, but from Fig. 13, it is evident that with higher starting conductances the response changes shape. In the discussion of paper II, we will argue that the change in shape is due to a process for which Mueller (1979) has a reasonable explanation.

I. Initial Responses to Monazomycin

The data we report in this section, in a strict sense, lie outside the scope of our theory. The kinetic equation pertains only to states of the system in which repeated voltage steps from some initial conductance reliably give rise to a particular steady-state conductance via a certain time course. Obviously, it is not applicable for the period of time between addition of monazomycin and the development of full sensitivity. (The effects described here are much too slow to have to do with stirring transients.)

This lack of correspondence between the formalism and the modification process is, paradoxically, implicit in the formalism. So far we have been discussing solutions of Eq. 6 which involve g approaching g_∞ so that $1 - (g/g_\infty)^B$ and therefore dg/dt goes to zero. There is, however, a second type of solution, namely where g is zero to start with. In this case, Eq. 6 is satisfied; moreover no mechanism is available to allow a jump in state to the first kind of solution. Taken at face value, the theory precludes the type of behavior it is designed to describe. Because the transition to finite conductance occurs, some additional interaction between monazomycin and the membrane must be possible.

FIGURE 13. Variation in the shape of a conductance increase as a function of the initial conductance. The seven conductance increases in the oscilloscope record are in response to voltage steps from $V = 0$ to $V = 30$ mV. The time spent at $V = 0$ was varied; from left to right the $V = 0$ time 5, 10, 15, 30, 60, (indeterminate) and 120 s. The "indeterminate" response is merely the first one at 30 mV after a complicated history. The seven responses, together with the interposed intervals at $V = 0$, were continuous in time; they were taken in order of increasing off-time after the achievement of the steady-state for the indeterminate response. Note that the initial conductance is highest after a short time spent at $V = 0$. Also, the responses do not superimpose just by translation along the time axis except for those after 60 and 120 s at $V = 0$. The monazomycin concentration was 2.0×10^{-6} g·ml^{-1}.

The meaning of this rather strange situation becomes clear if we introduce part of our molecular model now. We will argue that the existence of the growth portion of conductances rises and the dependence of the rate of growth on aqueous monazomycin concentration imply that monazomycin movements into and out of the membrane are autocatalyzed. By this we mean that the amount of monazomycin present in the membrane determines the rate at which it can enter or leave. Thus, if there is no monazomycin in the membrane, its rate of entry via this mechanism must be, identically, zero. Because some does get in after adding it to the aqueous solution, a noncatalyzed pathway must also exist.[6]

[6] We can also infer that the equilibrium for this pathway lies far toward the aqueous state of monazomycin, because the behavior of the membrane is dominated by the autocatalytic process once it is possible. The noncatalyzed pathway may depend on the insertion of "wrong-way" monazomycin (Results, part *F*) or on a mass action entry of "normal" monazomycin if V is made positive enough.

We have seen two distinguishable forms of the modification process, which we may refer to as "simple" and "drifting." The simple process may be characterized as follows: We add enough monazomycin to the *cis* solution so that our working conductance range (10^{-8}–10^{-6} Ω^{-1}) is reached with the 20-mV-stimulus range centered at ~60mV. If we wait ~15 min at $V = 0$ and then apply a 60-mV stimulus, the initial response will be of the sort we have been discussing. On the other hand, if we clamp the potential to 60 mV as soon as we have stopped stirring after addition of monazomycin, the membrane conductance will increase for 5 min or more before it stabilizes. If the first stimulus is applied at intermediate times, the approach to full sensitivity will be faster the closer to 15 min we wait. In this simple process, the development of full responsiveness may be hastened by imposing a higher than usual potential for a few seconds. In other words, if we were to clamp to, say, 120 mV for 5 s at 1 min after monazomycin addition and then switch to 60 mV, the conductance would decline and stabilize in the expected range in a few seconds. Returning to $V = 0$ and then testing with various steps would reveal the membrane to be fully sensitive.

Three examples of the type of conductance response seen during the drifting modification process are shown in Fig. 14; these are all taken at $V = 50$ mV. Each linear record (Fig. 14*a*) begins with the usual S-shaped conductance rise, but no steady-state is reached. Instead, the conductance creeps upward at a very slow rate. The drifting behavior is always associated with a conductance lower than that expected at the applied membrane potential when good steady states are achieved. The very slow climb of the conductance may go on for >30 min, and in addition cannot be accelerated very much by strong stimulation.

The relative insensitivity of the drift to applied potential can be seen in the logarithmic record (Fig. 14*b*). In spite of the two times that V was returned to zero, the slow phase of the conductance rise continues unabated. In other words, a straight-edge reveals that the slow rise of log I goes on at the same rate ($\tau = 165.0$ s) whether $V = 0$ or $V = 50$ mV. The same conclusion holds even if V is set to zero for longer times than in the record of Fig. 14.

The most obvious explanation of the drift is that it represents participation of a bigger and bigger fraction of the membrane area in the conductance response, but the log I record of Fig. 14 makes this untenable. As we have seen, log A is proportional to log g_∞, but if the membrane area is varied, only g_∞ (which is an extensive variable) should change; A (which is an intensive variable) should stay constant. Because A grows progressively for the three illustrated responses, we can infer that the drift is not just a reflection of the fraction of the thin phase which is modified. (We do not see any correlate of the drift when we visually monitor our membranes.) We think we can also preclude the idea that the drifting of the conductance is due to changes in the state of aggregation of the aqueous monazomycin (e.g., a slow breakup of large micelles) because we have seen cases in which a first film showed the simple process, whereas a second one painted in the presence of the same monazomycin exhibited the drift.

It is worth stating a few other characteristics of films that behaved in this rather complicated manner. First, and most important, if we allowed enough time to pass, many drifting membranes (and perhaps all, if we had had enough patience and stable enough membranes) reached full sensitivity and thereafter were indistinguishable from their simple counterparts. Second, elevating the temperature could sometimes rapidly get the membrane to full responsiveness. Third, the conductance during drifting was inordinately sensitive to mechanical perturbations of the system, such as stirring the solutions or tapping the chamber; the sign of the mechanically induced conductance change was usually but not always an increase. Fourth, cholesterol-free films

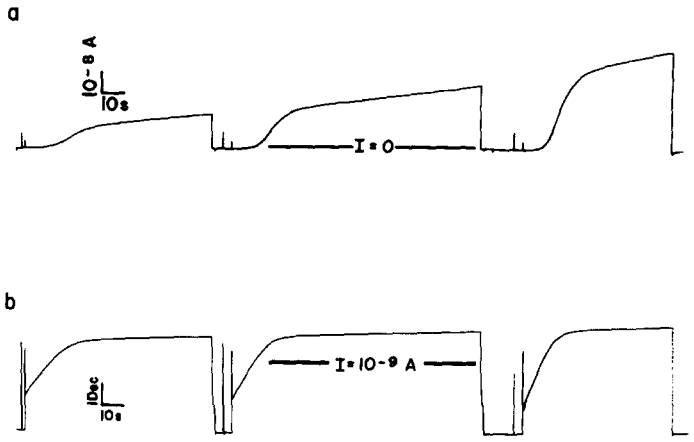

FIGURE 14. Examples of the altered shape of conductance increases seen during the drifting modification process. The record starts ~11 min after the addition of monazomycin and covers a total of 4.9 min. Each of the three responses follows a step from $V = 0$ to $V = 50$ mV; the potential was switched (as indicated by the capacitance spikes) to -100 mV for a few seconds between the 50-mV steps. Further description can be found in the text. The monazomycin concentration was 2×10^{-6} g·ml. The low-pass filter was set at 20 Hz.

on occasion exhibited drift, thus eliminating vagaries in the association of sterol and phospholipid as an explanation. Finally, the drift appears to be seasonal to some extent: it happens most often in spring and fall. Given this variation, it is hard to specify the fraction of films that drifted. At worst, we would find this behavior in all films for a week or two at a time; at best, it would be absent for weeks or months.

In the present work, the existence of this phenomenon was a rather severe annoyance, but actually it represents a fairly interesting topic for future consideration. We feel that is a genuine, if mysterious, property of the system because it shows translational invariance: we were able to observe it in a laboratory one borough removed from Brooklyn.

DISCUSSION

Probably the most important finding in this study is that the rate constant that characterizes the kinetics varies with the aqueous monazomycin concentration. Mueller (1979) observed a similar effect (although he defines his rate constant differently) and concluded that this was a virtual proof that several monomers or small oligomers must come together to form a channel. We agree with this view and, in fact, would like to state it even more strongly. The observation that the rate constant depends on modifier concentration seems to us to preclude the possibility that monazomycin channels are fixed, independent entities that are gated open or closed by membrane potential. In the cases of, for instance, the potassium channels of nerve membrane or excitability-inducing material (EIM) channels, one is dealing with populations of (probably) identical molecules whose kinetics properties are built-in features of each individual molecule. Thus, although the rate of switching state after a voltage step will depend on the number of channels in the membrane, the rate constant cannot. For such fixed channels, the rate constant is determined only by membrane potential. In contrast, no one-to-one mapping of rate constant onto membrane potential is possible for the monazomycin system. The rate of formation of channels is a mass-action property of monazomycin rather than an attribute of any single molecule.

An even strong conclusion can be drawn from this same observation. For the rate constant (as opposed to the rate itself) to depend on the monazomycin concentration there must be some autocatalytic step involved in channel formation. We define our rate constant as $A = \frac{1}{g}\frac{dg}{dt}$ (Eq. 7). If we assume that there is no autocatalytic step involved in the monazomycin conductance, then we may write a differential equation that describes the conductance increase at times small enough that the back reaction is insignificant:

$$\frac{dg}{dt} = k_1(V)[\text{Mon}]^s, \tag{21}$$

where $k_1(V)$ describes the voltage dependence of A. Thus,

$$g = k_1(V)[\text{Mon}]^s\, t. \tag{22}$$

Therefore,

$$A = \frac{k_1(V)[\text{Mon}]^s}{k_1(V)[\text{Mon}]^s\, t} = \frac{1}{t}. \tag{23}$$

In other words, assuming the validity of our definition of A, which we believe is the most "natural" one, a simple mass-action model which allows monomers to aggregate to channels yields a rate "constant" that is independent of [Mon] but that varies inversely with time. By contrast, an autocatalytic model, presented in detail in papaer II, allows A to be time invariant and [Mon]dependent. Thus, postulating autocatalysis is really just rephrasing the observation.

That there is an autocatalytic step may also be inferred directly from the growth region of conductance rises. The existence of an exponential growth characteristic for a population means that the instantaneous rate of increase of the population must be proportional to its size. Because we are loathe to postulate that monazomycin molecules are reproducing sexually or asexually, it must be that the concentration of some intramembrane monazomycin species determines the height of the energy barrier that other molecules must surmount to get to a state in which they, too, can aggregate to form channels.

The nonfirst-order kinetics of conductance decays can be understood directly from this point of view. If we assume that microscopic reversibility holds, then the rate constant that determines how fast monazomycin molecules can leave the activated state also depends on the intramembrane concentration of the catalyzing species. Thus as the conductance falls, so does the rate constant for further decreases. We postpone further considerations to paper II.

We thank Dr. O. S. Andersen for his help and interest, and Dr. Scott Berger for experimental contributions.

The computations in this paper were done on equipment supported by grant 5RO1 NS 10987 from the National Institutes of Health.

Received for publication 19 November 1980.

REFERENCES

AKASAKI, K., K. KARASAWA, M. WANATABE, H. YONEHARA, and H. UMEZAWA. 1963. Monazomycin, a new antibiotic produced by a streptomyces. *J. Antibiot. (Tokyo) Ser. A.* **16**:127.

ANDERSEN, O. S., A. FINKELSTEIN, I. KATZ, and A. CASS. 1976. Effect of phloretin on the permeability of thin lipid membranes. *J. Gen. Physiol.* **67**:749.

BAMBERG, E., and JANKO, K. 1976. Single channel conductance at lipid bilayer membranes in presence of monazomycin. *Biochim. Biophys. Acta* **426**:447.

HEYER, E. J., R. U. MULLER, and A. FINKELSTEIN. 1976. Inactivation of monazomycin-induced voltage-dependent conductance in thin lipid membranes. II. Inactivation produced by monazomycin transport through the membrane. *J. Gen. Physiol.* **67**:731.

HODGKIN, A. L., and A. F. HUXLEY. 1952. A quantitative description of membrane current and its application to conduction and excitation in nerve. *J. Physiol. (Lond.)*. **177**:500.

KOLB, H. A. 1979. Conductance noise of monazomycin-doped bilayers. *J. Membr. Biol.* **45**:277.

KUNZ, S. K. 1957. Numerical Analysis. McGraw-Hill, Inc., New York.

MOORE, L. E., and E. NEHER. 1976. Fluctuation and relaxation analysis of monazomycin-induced conductance in black lipid membranes. *J. Membr. Biol.* **27**:347.

MUELLER, P. 1979. The mechanism of electrical excitability in lipid bilayers and cell membranes. *In* The Neurosciences: Fourth Study Program. F.O. Schmitt and F.G. Worden, editors, The MIT Press, Cambridge, Mass. 641.

MUELLER, P., D. O. RUDIN, H. TiTIEN, and W. C. WESTCOTT. 1963. Methods for the formation of single biomolecular lipid membranes in aqueous solution. *J. Phys. Chem.* **67**:534.

MULLER, R. U., and O. S. ANDERSEN. 1975. Single monazomycin channels. Fifth International Biophysics Congress. Copenhagen. III. (Abstr.).

MULLER, R. U., and A. FINKELSTEIN. 1972*a*. Voltage-dependent conductance induced in thin lipid membranes by monazomycin. *J. Gen. Physiol.* **60:**263.

MULLER, R. U., and A. FINKELSTEIN. 1972*b*. The effect of surface charge on the voltage-dependent conductance induced in thin lipid membrane by monazomycin. *J. Gen. Physiol.* **60:**285.

MULLER, R. U., and C. S. PESKIN. 1981. The kinetics of monazomycin-induced voltage-dependent conductance. II. Theory and demonstration of a form of memory. *J. Gen. Physiol.* **78:**201–229.

WANKE, E., and G. PRESTIPINO. 1976. Monazomycin channel noise. *Biochim. Biophys. Acta.* **436:** 721.